January 1972

# Optimizing Resistance Coefficients for Large Bed Element Streams

D. E. Overton

Harl E. Judd

C. W. Johnson

# OPTIMIZING RESISTANCE COEFFICIENTS FOR LARGE BED ELEMENT STREAMS

By

D. E. Overton,
Harl E. Judd,
and
C.W. Johnson

Utah Water Research Laboratory
College of Engineering
Utah State University
Logan, Utah 84321

June 1972

PRWG59a-1

## ACKNOWLEDGMENTS

The work reported herein was carried out under cooperative agreement No. 12-14-100-9715 (41) between the Utah Water Research Laboratory and the Agricultural Research Service with funds from the Soil and Water Conservation Research Division, Northwest Watershed Research Center, Boise, Idaho, and USDA Hydrograph Laboratory, Beltsville, Maryland.

This report contains results from numerous field studies and from a laboratory study conducted by the authors at the Utah Water Research Laboratory during the summer of 1968.

D. E. Overton
Research Hydraulic Engineer
Southeast Watershed Research Center
USDA-ARS-SWC
Athens, Georgia

Harl E. Judd
Dean of Science
Southern Utah State College
Cedar City, Utah

C. W. Johnson
Supervisory Hydraulic Engineer
Northwest Watershed Research Center
USDA-ARS-SWC
Boise, Idaho

# TABLE OF CONTENTS

## LIST OF FIGURES

## LIST OF FIGURES (Continued)



## LIST OF TABLES

# OPTIMIZING RESISTANCE COEFFICIENTS FOR LARGE BED ELEMENT STREAMS

## Introduction

This is a report of a comparison of Darcy resistance coefficients calculated for previously reported laboratory data (5, 9, 13, 16) and those calculated for large bed element streams (7). Large bed element (LBE) streams exist frequently in nature where rocks derived from valley walls or from channels cutting through ancient glacial or fluvial deposits are moved only under conditions of extreme flood (7). The height of bed elements is a significant part of the mean depth of flow. The stream gradients are high and are quite stable for all but the highest flows.

The results of the analysis of Overton and Hamon (11) of previously reported data were embodied in a diagram relating the Darcy resistance coefficient to roughness intensity and the wall effect ratio (height of elements to width of flume). Plotting resistance coefficients calculated for the LBE stream data (7) on this diagram resulted in little agreement between the laboratory and field data. Some possible reasons for this disparity are considered.

Overton and Hamon (11) calculated significantly different Darcy resistance coefficients for two boundaries that had identical roughness intensities but different spacings. In contrast, Judd and Peterson (7) found a unique relation between roughness intensity and the average spacing of steps or overfalls in LBE streams formed by the accumulation of smaller elements around larger elements. In an attempt to further clarify the effect of spacing on resistance, the writers of this report undertook a study at the Utah Water Research Laboratory. They found that random arrangements of roughness elements produced markedly higher head losses than regular diamond shaped patterns with the same roughness intensity. The resistance coefficients calculated from the previously reported laboratory data by Overton and Hamon (11) reached a maximum for roughness intensities between 0.1 and 0.2. Most of the LBE streams studied by Judd and Peterson (7) were in this range of roughness intensity. It seems possible that nature may arrange LBE material in an optimal way; i.e. producing a roughness intensity associated with a maximum resistance. In the design of future studies, this comparison of laboratory and field data may be useful in refining present concepts of similarity. To that end, the relation between roughness intensity and step spacing for LBE streams developed by Judd and Peterson (7) may provide the most up-to-date quantification of the geometric similarity between LBE streams and laboratory models.

## Definition of Resistance Coefficient

Prediction of resistance coefficients for unlined channels is now essentially an art (4). The ASCE Task Force on Friction Factors in Open Channels (3) attempted to make available a resistance diagram similar to the one used for steady flow in pipes. The Task Force concluded that such an ultimate goal was not attainable with the present state of knowledge.

The analysis of Overton and Hamon (11) was an attempt to attain such a procedure. They examined previously-reported laboratory flows over cubes, sheet metal baffles, and square steel strips. They found that one of the main problems preventing the development of a general resistance diagram was the lack of uniformity in the assumption of the location of the plane of effective zero velocity. Because velocity profiles are usually not available, the location of the zero velocity plane at some distance, $\epsilon$, above the flume floor must be assumed. Even in the presence of finite roughness elements in dense concentrations, some have assumed that the plane was located at the bottom of the flume. Others have assumed that the location of the zero plane was at a height above the flume floor that would theoretically result from a melting down of all of the roughness elements for sparse patterns and at a height equal to the top of the roughness elements for densely spaced elements. Also, these previously reported studies have tacitly assumed that the assumption of the location of the zero plane would not significantly affect the resulting relation between the resistance coefficient and Reynolds number.

Overton and Hamon (11) found that the relation between resistance coefficient and associated Reynolds numbers was extremely sensitive to the assumption of the location of the plane of effective zero velocity. In some instances, raising the assumed plane only 0.01 foot caused a decrease in the Darcy resistance coefficient of more than

100 percent at low flows. For many roughness patterns the Darcy resistance coefficient became almost invariant with Reynolds number if the zero plane was assumed to be at the top of the roughness elements. This is essentially what Koloseus and Davidian (9) found for their very dense pattern of elements. Because of the sensitivity of this relation, and the uncertainty of the location of the zero velocity plane, a systematic procedure was developed for locating this plane.

The discharge per unit width of channel is defined as

$$Q/w = \int_{\epsilon}^{y} v \, dy_i \quad \ldots\ldots\ldots \quad (1)$$

in which Q is discharge, w is width of the channel, v is point velocity associated at a depth $y_i$ above the flume floor. From Equation 1 the average velocity is

$$V = Q/w(y - \epsilon) \quad \ldots\ldots\ldots\ldots \quad (2)$$

The Darcy-Weisbach formula adapted to open channel flow is

$$V = \sqrt{\frac{8g}{f}} \sqrt{RS} \quad \ldots\ldots\ldots \quad (3)$$

in which f is the resistance coefficient, R is the hydraulic radius, S is the slope of the energy gradient, and g is gravitational acceleration. The hydraulic radius is defined as the cross sectional area of flow divided by the wetted perimeter.

$$R = \frac{w(y - t)}{w + 2(y - \epsilon)} \quad \ldots\ldots\ldots \quad (4)$$

The final form of the Darcy-Weisbach formula results when Equations 2 and 4 are combined into Equation 3 to obtain

$$Q = \sqrt{\frac{8g}{f}} \, w(y - \epsilon) \sqrt{\frac{w(y - \epsilon)}{w + 2(y - \epsilon)} S} \quad \ldots \quad (5)$$

To illustrate the sensitivity of the resistance relation with $\epsilon$, resistance coefficients were calculated from Equation 5 for selected values of $\epsilon$ for the data reported by Ragan (14). These data were obtained from a 72-foot rectangular flume, 8 inches wide. The flume was roughened with ¼-inch (.0208 ft.) angle aluminum strips which were cemented to the bottom and sides of the flume at 1-foot intervals. The slope of the flume was held at 0.2 percent for all flows. Since there were no velocity profiles, the location of the zero plane has to be assumed. There is only one equation, Equation 5, but two unknowns, f and $\epsilon$.

In this illustration, the writers assumed that the height of the zero plane was 0, 0.015, and 0.030 foot above the flume floor. The f-values for each of the seven normal flows reported by Ragan for each assumed value of $\epsilon$ and the associated Reynolds numbers are plotted in Figure 1 where

$$R_e = \frac{Q/\nu}{w + 2(y - \epsilon)} \quad \ldots\ldots\ldots \quad (6)$$

and $\nu$ is kinematic viscosity. Moving the plane up or down slightly resulted in substantially different resistance relationships. Not knowing what the true relation is, the $\epsilon$-value that produced a constant resistance coefficient was calculated. If, in fact, the resistance coefficient were invariate with Reynolds number, flows would be in the classical hydrodynamically rough region of the Moody diagram for pipe flow. If f-values, relative roughness values, and Reynolds numbers were in the hydrodynamically rough region, verification of such a direct analogy could only be accomplished by operating on velocity profiles, but these are not available.

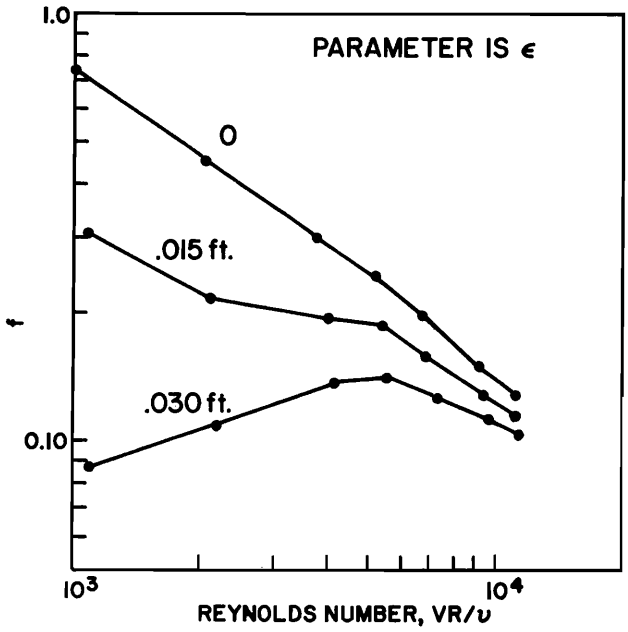


**Figure 1. f versus Reynolds number for Ragan flume—parameter is $\epsilon$.**

This apparent dilemma can be resolved if the plane of zero velocity is calculated in an objective manner. If the zero plane that produces a constant resistance coefficient is sought, two important advantages will accrue. First, all analysts will determine the plane of zero velocity at the same elevation, and the same resistance relationship will result. Second, treating the resistance

coefficient as a constant makes the analysis much easier. Also, flows in the field are seldom steady and uniform, therefore, a simplified approach such as this one seems fully justified by practical considerations.

Instead of plotting f-values versus Reynolds number and searching for the plane of zero velocity, as was done here with the Ragan data, a more efficient and objective procedure is suggested. The overall goal is to predict with minimum error the discharge for a given depth of flow. It was found to be much simpler with no loss in generality to minimize the error in predicting conveyance ($K = Q/\sqrt{S}$) rather than discharge. The objective function is then

$$\text{Minimize} \left\{ \sum_{1}^{N} [K - \hat{K}]^2 \right\} \quad \ldots\ldots (7)$$

where N is the number of observations of steady uniform flow over a roughness boundary, K is observed conveyance and $\hat{K}$ is predicted conveyance from Equation 5. Optimum values of the roughness parameter, $\epsilon$, and the Darcy resistance coefficient were computed by a least squares fit to an implicit mathematical model. Inserting the relation for conveyance from Equation 5 into the objective function, Equation 7, results in

$$f = \frac{\Sigma K^2 - [\Sigma A \sqrt{8gR}]^2/N}{\Sigma KA \sqrt{8gR} - \overline{K} \Sigma A \sqrt{8gR}} \quad \ldots\ldots (8)$$

where $\overline{K}$ is the mean conveyance. Conveyance is correlated line only with $A\sqrt{8gR}$, from physical considerations this must have a zero intercept on the ordinate axis. The coefficient $1/\sqrt{f}$ would therefore be the resulting slope of the regression line, thus

$$0 = \Sigma K - \frac{1}{\sqrt{f}} \Sigma A \sqrt{8gR} \quad \ldots\ldots (9)$$

The resistance coefficient was eliminated from Equations 8 and 9 resulting in a new equation with $\epsilon$ as the only unknown.

$$\phi(\epsilon) = \Sigma KA \sqrt{8gR} - \Sigma K \Sigma A^2 8gR = 0 \quad \ldots\ldots (10)$$

An explicit equation for $\epsilon$ cannot be obtained; however, Equation 10 must be solved for $\epsilon$ by the Newton-Raphson iterative technique. Roughness parameter was successively approximated by

$$\epsilon_{i+1} = \epsilon_i - \frac{\phi(\epsilon_i)}{\phi^1(\epsilon_1)} \quad \ldots\ldots (11)$$

in which i is the iteration number. The value of the roughness parameter $\epsilon_{i+1}$ was accepted when

$$\left| \frac{\epsilon_{i+1} - \epsilon_i}{\epsilon_i} \right| < 0.005 \quad \ldots\ldots (12)$$

The value of the resistance coefficient was calculated using either Equation 8 or Equation 9.

## Analysis of Previously Reported Data

The Ragan flume solution value for f was 0.125 and for $\epsilon$ 0.030 ft. Percent standard error in fitting conveyance was only 6.3 percent. In Figure 2 conveyance has been plotted against $A\sqrt{8gR}$ for $\epsilon$ equal to 0 and 0.030 ft. The latter value of the roughness parameter $\epsilon$ forced the regression line through the origin. The slope of the line was $1/\sqrt{f}$.

Data reported by Koloseus and Davidian (9), Powell (13), and Sayre and Albertson (16) were also analyzed. Constant resistance coefficients and roughness parameters were derived for a total of 26 roughness patterns involving 917 steady uniform flows. The derived constant resistance coefficients were plotted against associated roughness intensities in Figure 3 (the sum of the total projected area of roughness elements in the direction of flow divided by the total area of the floor). The points in Figure 3 were labeled by the ratio of the height of the roughness elements divided by the width of the flume, an attempt to account for the wall effect relative to the roughness elements. For a given roughness intensity, the resistance coefficient increased as the wall effect ratio increased. As this ratio approaches zero, one dimensional flow is approached.

## Observations and Analysis of Judd and Peterson

Judd and Peterson (7) analyzed flows from 15 LBE natural channel sites located in Utah, Colorado, and New Mexico. They defined LBE channels as streams having sufficiently large slopes to cause gravitational surface disturbances at some stages of discharge and roughness material occupied a significant portion of the depth of flow. The term LBE was used rather than roughness because more than just surface drag or friction was involved in the head losses. Flow deformations resembled channel changes and additional head losses were caused by spills. "High-gradient" instead of "steep" was used because steep channels are usually associated with supercritical flow, and the observed flows in LBE channels were usually subcritical. A small statistical sample of channel and flow variables had been taken and it was necessary to average in order to obtain "macroscopic" uniform flow.

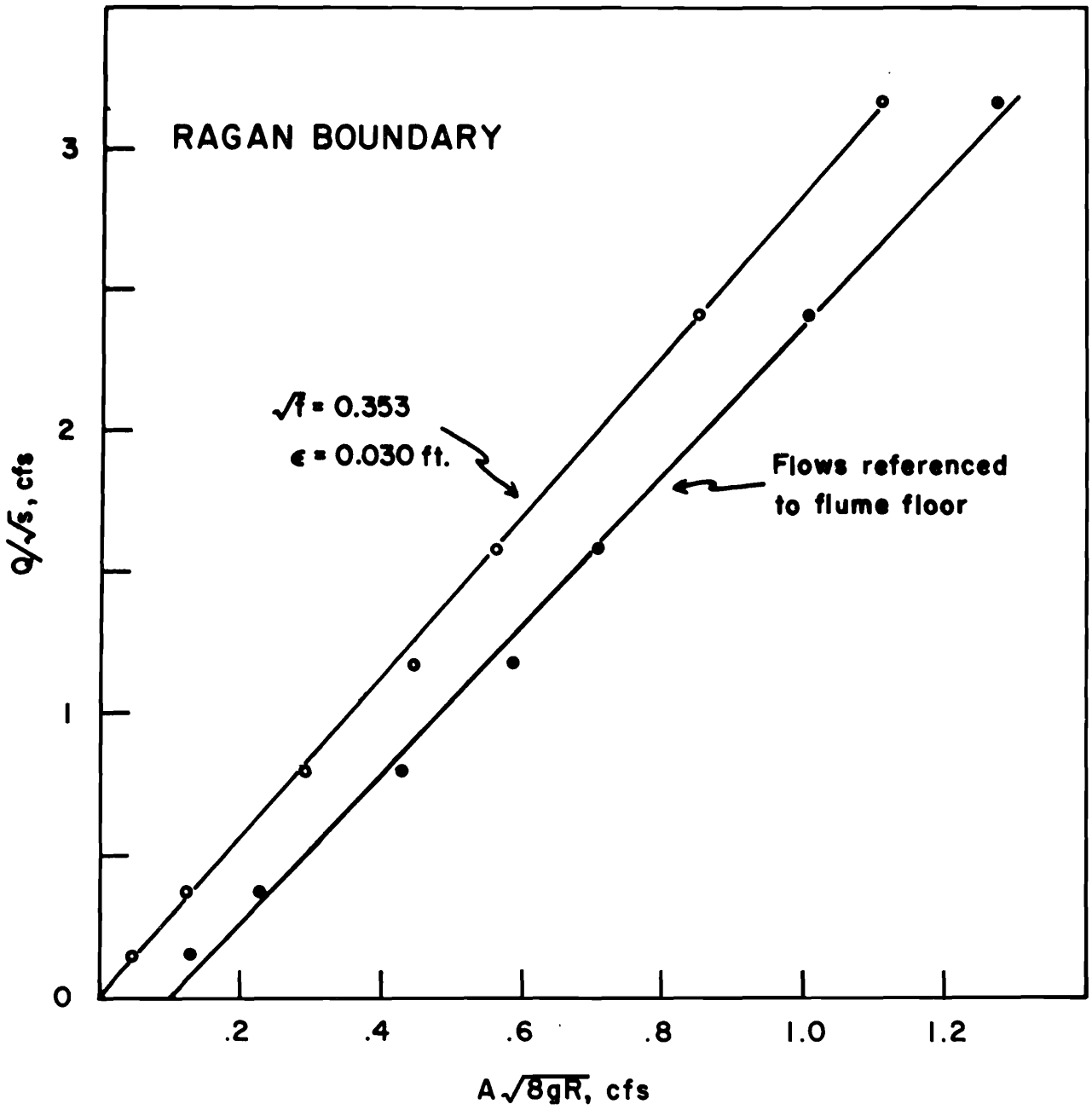


**Figure 2. $Q/\sqrt{S}$ versus $A\sqrt{8gR}$ for Ragan flume.**

One must keep in mind that the constant resistance coefficients suggested by the writers are rough averages. Nevertheless, such an approach is justified in view of the general lack of large and detailed samples of all of the variables involved. As a guide in the quantification there are several important observations that have been made.

Peterson and Mohanty (12) based on flume experiments and visual observations of natural streams have identified three distinct regimes of flow in LBE streams: tranquil, tumbling, and rapid. These flows are described as follows:

(1) Tranquil flow occurs only on streams of about 3 percent slope or less, and the depth of flow is greater than critical depth. The free surface is usually smooth.

(2) Tumbling flow is characterized by supercritical flows over some of the elements returning to subcritical flow after a dissipative hydraulic jump.

(3) Rapid flow is generally supercritical throughout and the water tends to skim over the elements. Horizontal vortices may occur in between the elements.

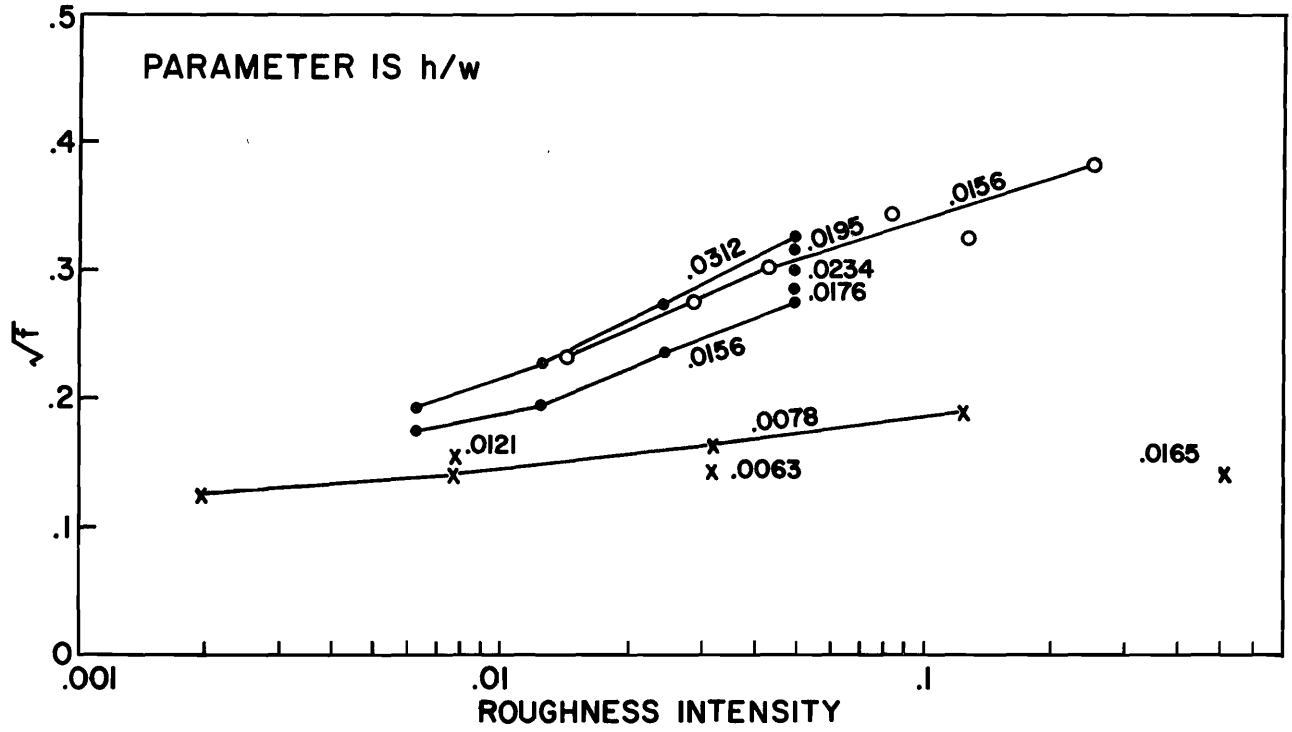


**Figure 3. $\sqrt{f}$ versus roughness intensity–parameter is h/w.**

Each of the regimes represents a distinctly different hydrodynamic condition. These brief descriptions of the regimes of flow should well illustrate that associating a single resistance coefficient for all flows is indeed an average, since the three regimes may occur at a stream site as discharge changes.

Judd and Peterson (7) observed that average velocities in LBE streams were usually subcritical even at high stages. Based upon this observation, it can be shown that there is a lower limit to the resistance coefficient. From Equation 3 the Froude number can be shown to be

$$F = \frac{V}{\sqrt{gR}} = \sqrt{\frac{8S}{f}} \quad \ldots\ldots\ldots (13)$$

If flows are usually in the subcritical range, the Froude number is less than 1. It follows that the resistance coefficient will be greater than 8S, or

$$f > 8S \quad \ldots\ldots\ldots\ldots\ldots (14)$$

In a series of flume experiments of self-formed LBE beds at the Utah Water Research Laboratory, Hariri (6) held discharge constant and gradually increased the slope of the flume. As the Froude number approached 1.0 the larger elements began to move but the Froude number did not exceed 1.0. Judd and Peterson (7) reasoned that scour action would be increased greatly at flows nearly critical because of increasing drag forces associated with gravity waves. This system of standing waves appeared to them to strengthen the formation of combinations of roughness elements (transverse bars or aggregates of boulders) so rapidly that velocities in excess of critical are unlikely to occur in self-scoured LBE streams. This is offered as an explanation of the physics behind Inequality 14.

As velocity increases the scouring of the stream increases, and only the larger bed elements are not displaced. For the same bed forming discharge, it takes a greater projected area (roughness intensity) to resist flow in steeper channels than in flatter channels. Therefore, roughness intensity should be a function of channel slope.

$$\theta = \theta(S) \quad \ldots\ldots\ldots\ldots\ldots (15)$$

where $\theta$ is roughness intensity. Figure 4 was taken from their report and shows roughness intensity and associated bed slope of the LBE streams studied by them and the laboratory data of Hariri (6). They separated the LBE data into three groups:

(1) Narrow channels with large elements protruding from the walls.
(2) Wider channels with less wall resistance.
(3) Much wider channels with less wall resistance.

Hariri's channels had the least wall resistance because of the absence of vegetation on the banks and the fact that the bed forming material was completely granular. The results were generalized as

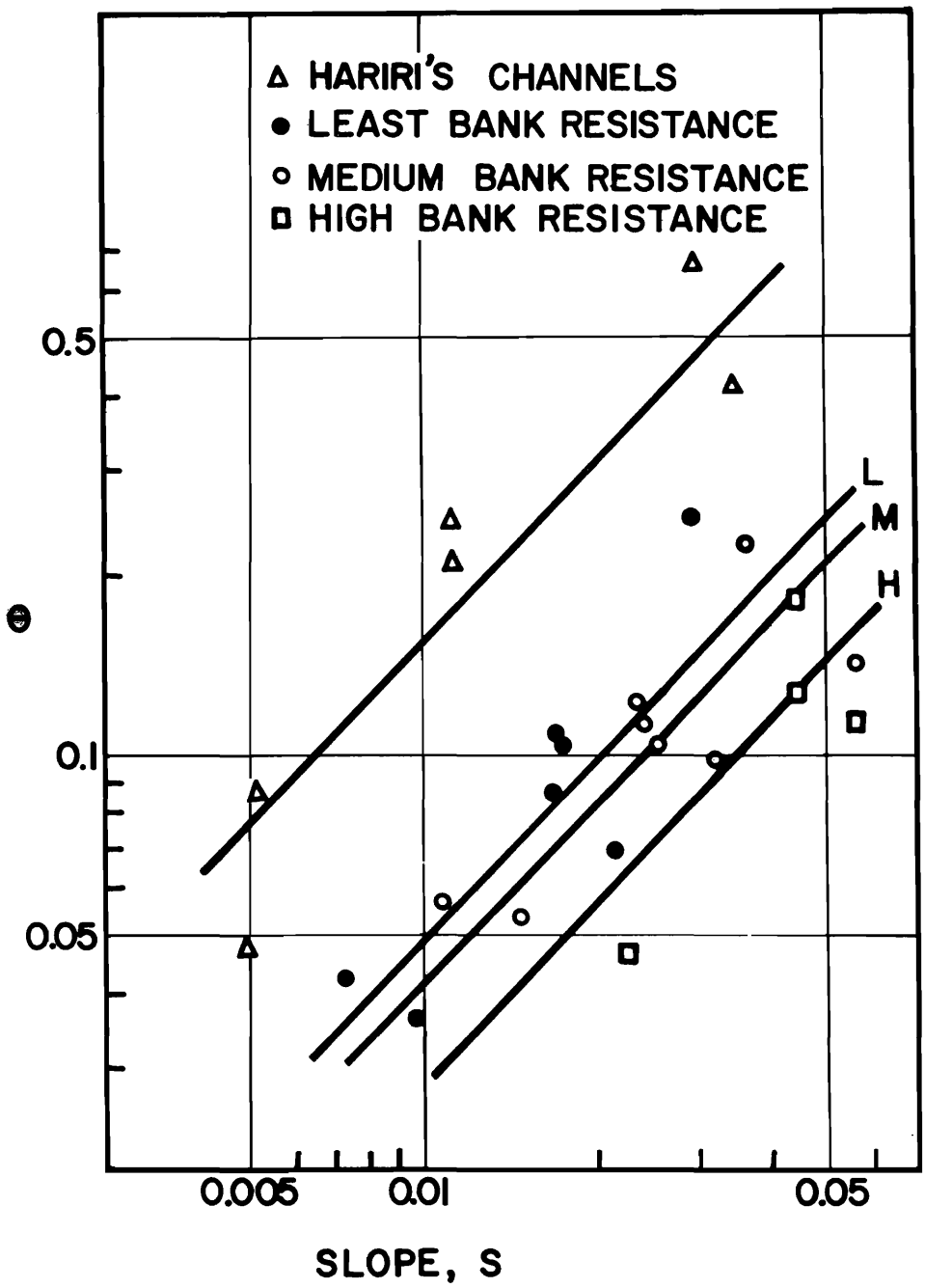


**Figure 4. Roughness intensity versus bed slope for LBE streams–after Judd and Peterson (9).**

$$S = B\theta \quad \ldots\ldots\ldots\ldots (16)$$

where B is a constant that depends upon the influence of the channel banks, and gradation and shape characteristics of the LBE. For the case of least or zero bank resistance in LBE channels, the B-value approached 0.2.

These sources provide enough information to estimate the minimum f-value of a LBE stream. This minimum f-value can be expressed in terms of the size, shape, and intensity of the LBEs. For example, take the case of a wide channel. Combining Equation 16 for B equal to 0.2 with the Inequality 14 results in

$$f > 1.6\theta \quad \ldots\ldots\ldots\ldots (17)$$

Judd and Peterson (7) have offered an explanation of the basic channel forming process which produces the roughness intensity of a LBE channel. They observed that in most streams having a channel slope greater than 1

percent, bed element configurations in the form of steps or bars existed. They theorized that the steps began forming at high discharges. Somewhere in the channel there is a large rock that cannot be moved except at high discharges. Smaller elements begin to accumulate around the larger elements until a small dam or overfall results. This action tends to help form similar steps downstream and the deposition that results from the local scour causes a sequence of these steps at rather close spacings.

Field observations showed step spacing to follow the general relation,

$$L = k_{16}/CS \quad \ldots\ldots\ldots\ldots (18)$$

in which $k_{16}$ is a representative size of the LBE, L is the distance between steps, and C is a coefficient related to the stream. For streams where the slope was greater than 1 percent, which comprised most of the LBE streams studied, step formation is a significant factor in the morphology of roughness intensity.

Upon examining Equations 16 and 18 they developed an important relation between roughness intensity, step spacing and the size of the material.

$$\theta = \frac{k_{16}}{CBL} \quad \ldots\ldots\ldots\ldots (19)$$

Equation 19 could qualify as a working "law" of fluvial morphology of LBE streams. It shows that the relation between the size and intensity of roughness material is related in a unique manner to the spacing of the roughness material. The relation was essentially constant for any particular stream reach but varies somewhat from stream to stream depending upon the influence of channel banks, gradation, and shape characteristics of the streams. Attempts to simulate such flows had been made earlier at the Utah Water Research Laboratory by Mohanty (10) and by Al-Khafaji (2) using bar roughness elements placed perpendicular to the direction of flow.

An examination of the photographs in the Judd-Peterson report shows that steps are not as idealized as in the laboratory studies of bar roughnesses. Rather, steps or little dams are staggered in somewhat of a statistical fashion. The laboratory work would be fully justified because of the need to develop hypotheses for field testing. However, hindsight suggests that a working law such as that of Equation 19 should be observed in order to design the most realistic laboratory study within the framework of present knowledge.

The wall effect is important also. It would be desirable to simulate resistance coefficients in the laboratory which would be in the immediate range of observed resistance coefficients. Judd and Peterson (7) have provided a guide for designing such a study. By combining Equation 19 with Inequality 17 the wall effect has been shown to be an important factor affecting stream coefficients C and B. Therefore,

$$f > \frac{1.6\, k_{16}}{CBL} \quad \ldots\ldots\ldots\ldots (20)$$

in simulating field conditions in the laboratory, the right-hand side of Inequality 20 can be manipulated in order to develop similar resistance coefficients in laboratory studies.

In an attempt to supplement Inequality 20, a laboratory experiment was performed in the present study with the intent of comparing the effects of regular spacings and random spacings of bed elements on resistance. Such information is needed in order to improve present concepts of similarity between field and laboratory conditions.

## Laboratory Study of Roughness Spacing

Laboratory tests were made in an adjustable slope flume with plexi-glass walls and a steel floor located in the Utah Water Research Laboratory. The flume was 3 feet wide and 24 feet long. Water surface levels were read by point gages from a mobile carriage mounted on the flume walls. Discharge was measured by a precalibrated Parshall flume in the exit channel and checked by 25,000-pound-capacity weighing tanks. Depth of flow was regulated by an adjustable tailgate.

Because it was difficult to detect normal depth, the iterative procedure reported by Tracy and Lester (17) was used. A search was made for backwater and drawdown profiles with the least curvature. This was a process of setting the tailgate, measuring profiles, and resetting the tailgate in an attempt to straighten the previous profile. These profiles were plotted and normal depth was determined by interpolation.

Artificial roughness elements in the shape of hemispheres 3-5/8 inches in diameter were molded with a mixture of sand, marine plastic, and a suitable catalyst. Machine screws were set into the mold for attaching the hemispheres to plywood sheets.

Ten roughness patterns were designed—seven regular and three random. Regular patterns were formed in the shape of diamonds as shown in Figure 5. Each of these patterns was 3 feet long and was repeated eight times. Basic geometric data for the patterns are listed in Table 1. Patterns 2 and 3 have the same number of roughness elements in 24 feet but have markedly different spacings. The same is true for patterns 4 and 5, and for patterns 6 and 7.

In developing the random patterns, a 12-foot plywood slab was divided into 64 9-inch squares. A two

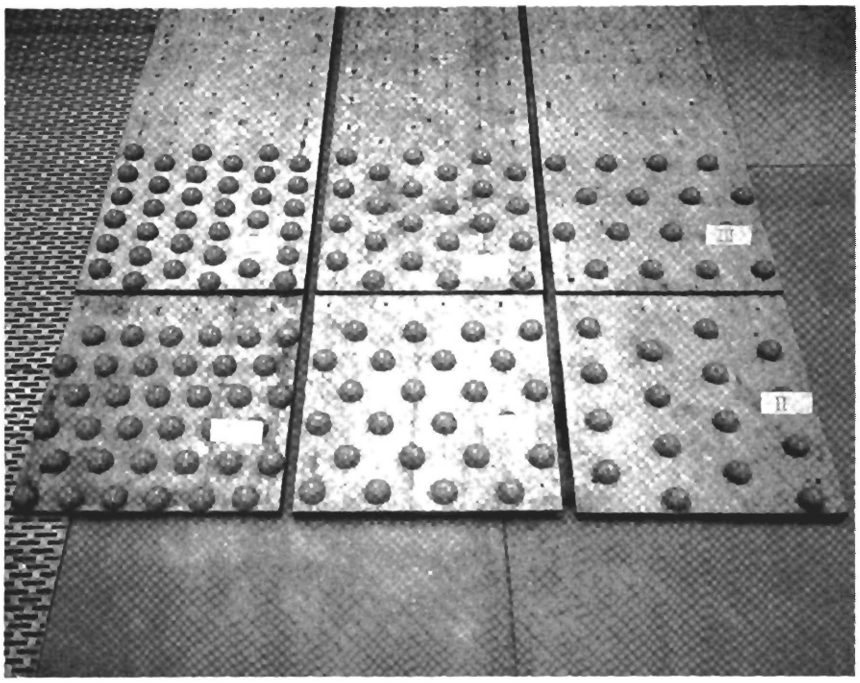

**Figure 5. Regular roughness patterns studied, Utah Water Research Laboratory, July 1968.**

**Table 1. Geometric data for roughness patterns (Overton, Judd and Johnson).**

| Pattern No. | Hemispheres in 24 ft. | Roughness Intensity | Spacing | | Spacing Parameter (x+e)/h |
|---|---|---|---|---|---|
| | | | Between x (long) | Centers e (trans.) | |
| | | | inches | | |
| Regular | | | | | |
| 1 | 64 | .0322 | 9 | 18 | 14.91 |
| 2 | 128 | .0645 | 4.5 | 18 | 12.43 |
| 3 | 128 | .0645 | 9 | 9 | 9.94 |
| 4 | 192 | .0966 | 6 | 9 | 8.29 |
| 5 | 192 | .0966 | 4.5 | 12 | 9.11 |
| 6 | 288 | .145 | 5.88 | 5.88 | 6.55 |
| 7 | 288 | .145 | 3 | 12 | 8.29 |
| Random | | | | | |
| 8 | 128 | .0645 | --- | --- | 8.50 [a] |
| 9 | 192 | .0966 | --- | --- | 7.05 [a] |
| 10 | 288 | .145 | --- | --- | 6.20 [a] |

[a]Equivalent spacing parameter.

Equation 21 has been used as an exact similarity criteria, but rather for the purpose of comparing the roughness patterns simulated in the flume with the general morphological observations that have been made of LBE streams. A summary of the flow data collected from these patterns is shown in Table 2, and computed results are shown in Table 3.

Regular patterns 2 and 3, and random patterns 8 had the same roughness intensity (0.0645 or 128 elements in 24 feet); regular patterns 4 and 5, and random pattern 9 had the same roughness intensity (0.0966 or 192 elements in 24 feet; and, regular patterns 6 and 7, and random pattern 10 had the same roughness intensity (0.145 or 288 elements in 24 feet). The spacing of regular

**Table 2. Flow data (Overton, Judd and Johnson).**

| Pattern No. | Run No. | Q cfs | y ft. | S % | Re[a] x10$^{-5}$ | F |
|---|---|---|---|---|---|---|
| | | | (Regular Patterns) | | | |
| 1 | 0101 | 0.558 | 0.211 | 0.50 | 0.122 | 0.803 |
| | 0102 | 0.776 | 0.245 | 0.50 | 0.166 | 0.803 |
| | 0103 | 0.976 | 0.268 | 0.50 | 0.206 | 0.803 |
| | 0104 | 1.200 | 0.298 | 0.50 | 0.249 | 0.803 |
| | 0105 | 1.380 | 0.316 | 0.50 | 0.283 | 0.803 |
| 2 | 0201 | 1.23 | 0.280 | 0.75 | 0.257 | 0.844 |
| | 0202 | 0.894 | 0.245 | 0.75 | 0.191 | 0.844 |
| | 0203 | 0.565 | 0.210 | 0.75 | 0.123 | 0.844 |
| | 0204 | 1.59 | 0.368 | 0.50 | 0.316 | 0.689 |
| | 0205 | 1.23 | 0.318 | 0.50 | 0.252 | 0.689 |
| | 0206 | 0.937 | 0.286 | 0.50 | 0.195 | 0.689 |
| | 0207 | 0.580 | 0.230 | 0.50 | 0.125 | 0.689 |
| 3 | 0301 | 1.44 | 0.370 | 0.50 | 0.288 | 0.643 |
| | 0302 | 1.26 | 0.345 | 0.50 | 0.255 | 0.643 |
| | 0303 | 1.00 | 0.306 | 0.50 | 0.207 | 0.643 |
| | 0304 | 0.774 | 0.272 | 0.50 | 0.163 | 0.643 |
| | 0305 | 0.648 | 0.254 | 0.50 | 0.138 | 0.643 |
| | 0306 | 0.502 | 0.230 | 0.50 | 0.109 | 0.643 |
| 4 | 0401 | 0.440 | 0.211 | 0.75 | 0.0967 | 0.669 |
| | 0402 | 0.598 | 0.239 | 0.75 | 0.129 | 0.669 |
| | 0403 | 0.882 | 0.273 | 0.75 | 0.186 | 0.669 |
| | 0404 | 0.440 | 0.236 | 0.50 | 0.0953 | 0.546 |
| | 0405 | 0.598 | 0.269 | 0.50 | 0.126 | 0.546 |
| | 0406 | 0.882 | 0.318 | 0.50 | 0.181 | 0.546 |
| | 0407 | 1.08 | 0.351 | 0.50 | 0.218 | 0.546 |
| | 0408 | 1.34 | 0.403 | 0.50 | 0.263 | 0.546 |
| | 0409 | 1.63 | 0.438 | 0.50 | 0.314 | 0.546 |
| | 0410 | 1.87 | 0.468 | 0.50 | 0.354 | 0.546 |
| | 0411 | 2.07 | 0.478 | 0.50 | 0.390 | 0.546 |
| 5 | 0501 | 0.397 | 0.203 | 0.75 | 0.0877 | 0.714 |
| | 0502 | 0.654 | 0.239 | 0.75 | 0.141 | 0.714 |
| | 0503 | 0.875 | 0.268 | 0.75 | 0.185 | 0.714 |
| | 0504 | 0.397 | 0.221 | 0.50 | 0.0867 | 0.583 |
| | 0505 | 0.654 | 0.270 | 0.50 | 0.138 | 0.583 |
| | 0506 | 0.875 | 0.308 | 0.50 | 0.181 | 0.583 |
| | 0507 | 1.08 | 0.340 | 0.50 | 0.219 | 0.583 |
| | 0508 | 1.29 | 0.372 | 0.50 | 0.257 | 0.583 |
| | 0509 | 1.54 | 0.407 | 0.50 | 0.302 | 0.583 |
| | 0510 | 1.71 | 0.436 | 0.50 | 0.330 | 0.583 |
| | 0511 | 1.95 | 0.448 | 0.50 | 0.373 | 0.583 |

*\continued*

Table 2. Continued.

| Pattern No. | Run No. | Q cfs | y ft. | S % | Re[a] x10$^{-5}$ | F |
|---|---|---|---|---|---|---|
| 6 | 0601 | 0.475 | 0.235 | 1.0 | 0.103 | 0.662 |
| | 0602 | 0.473 | 0.245 | 0.75 | 0.102 | 0.573 |
| | 0603 | 0.900 | 0.312 | 0.75 | 0.186 | 0.573 |
| | 0604 | 0.680 | 0.280 | 0.75 | 0.143 | 0.573 |
| | 0605 | 0.473 | 0.245 | 0.50 | 0.102 | 0.468 |
| | 0606 | 0.695 | 0.310 | 0.50 | 0.144 | 0.468 |
| | 0607 | 0.900 | 0.351 | 0.50 | 0.182 | 0.468 |
| | 0608 | 1.17 | 0.406 | 0.50 | 0.230 | 0.468 |
| | 0609 | 1.39 | 0.429 | 0.50 | 0.270 | 0.468 |
| | 0610 | 1.71 | 0.488 | 0.50 | 0.321 | 0.468 |
| 7 | 0701 | 1.03 | 0.330 | 0.75 | 0.212 | 0.712 |
| | 0702 | 2.00 | 0.454 | 0.75 | 0.384 | 0.712 |
| | 0703 | 3.06 | 0.551 | 0.75 | 0.558 | 0.712 |
| | 0704 | 4.03 | 0.633 | 0.75 | 0.706 | 0.712 |
| | 0705 | 5.04 | 0.734 | 0.75 | 0.841 | 0.712 |
| | 0706 | 6.34 | 0.822 | 0.75 | 1.01 | 0.712 |
| | 0707 | 1.03 | 0.380 | 0.50 | 0.206 | 0.581 |
| | 0708 | 2.00 | 0.543 | 0.50 | 0.366 | 0.581 |
| | 0709 | 3.06 | 0.651 | 0.50 | 0.531 | 0.581 |
| | 0710 | 4.03 | 0.763 | 0.50 | 0.663 | 0.581 |
| | | | (Random Patterns) | | | |
| 8 | 0801 | 0.437 | 0.201 | 0.75 | 0.0973 | 0.693 |
| | 0802 | 1.64 | 0.411 | 0.50 | 0.322 | 0.566 |
| | 0803 | 1.41 | 0.381 | 0.50 | 0.282 | 0.566 |
| | 0804 | 1.10 | 0.331 | 0.50 | 0.226 | 0.566 |
| | 0805 | 0.891 | 0.296 | 0.50 | 0.187 | 0.566 |
| | 0806 | 0.649 | 0.259 | 0.50 | 0.139 | 0.566 |
| | 0807 | 0.437 | 0.214 | 0.50 | 0.0965 | 0.566 |
| 9 | 0901 | 0.456 | 0.233 | 0.50 | 0.0572 | 0.503 |
| | 0902 | 0.712 | 0.279 | 0.50 | 0.148 | 0.503 |
| | 0903 | 0.866 | 0.300 | 0.50 | 0.178 | 0.503 |
| | 0904 | 1.11 | 0.346 | 0.50 | 0.226 | 0.503 |
| | 0905 | 1.36 | 0.399 | 0.50 | 0.265 | 0.503 |
| | 0906 | 1.59 | 0.426 | 0.50 | 0.305 | 0.503 |
| | 0907 | 0.456 | 0.209 | 0.75 | 0.0993 | 0.616 |
| | 0908 | 0.712 | 0.249 | 0.75 | 0.151 | 0.616 |
| 10 | 1001 | 0.406 | 0.223 | 0.75 | 0.0519 | 0.561 |
| | 1002 | 0.644 | 0.266 | 0.75 | 0.137 | 0.561 |
| | 1003 | 0.813 | 0.296 | 0.75 | 0.170 | 0.561 |
| | 1004 | 0.406 | 0.249 | 0.50 | 0.0873 | 0.458 |
| | 1005 | 0.644 | 0.303 | 0.50 | 0.134 | 0.458 |
| | 1006 | 0.813 | 0.333 | 0.50 | 0.166 | 0.458 |
| | 1007 | 1.083 | 0.386 | 0.50 | 0.215 | 0.458 |
| | 1008 | 1.303 | 0.422 | 0.50 | 0.253 | 0.458 |
| | 1009 | 1.625 | 0.475 | 0.50 | 0.307 | 0.458 |

[a]Water-temperature 50°F for all flows
Kinematic viscosity = 1.41 x 10$^{-5}$

Table 3. Results of resistance analysis (Overton, Judd and Johnson).

| Pattern No. | Number of Observations | Sp. Par (x-e)/h | $\sqrt{f}$ | $\epsilon$ ft. | Standard[b] Error % |
|---|---|---|---|---|---|
| 1 | 5 | 14.91 | 0.249 | 0.0913 | 6.3 |
| 2 | 7 | 12.43 | 0.290 | 0.0882 | 14.1 |
| 3 | 6 | 9.94 | 0.311 | 0.0972 | 4.5 |
| 4 | 11 | 8.29 | 0.366 | 0.0988 | 13.4 |
| 5 | 11 | 9.11 | 0.343 | 0.0988 | 10.9 |
| 6 | 10 | 6.55 | 0.427 | 0.104 | 10.9 |
| 7 | 10 | 8.29 | 0.344 | 0.109 | 10.0 |
| 8 | 7 | 8.50[a] | 0.353 | 0.0861 | 4.5 |
| 9 | 8 | 7.05[a] | 0.397 | 0.0811 | 8.9 |
| 10 | 9 | 6.20[a] | 0.436 | 0.101 | 6.3 |
| | 84 | | | | |

[a]Equivalent spacing parameter determined from Figure 9.

[b]Avg. strd. error = 9.4%.

patterns that had the same roughness intensities differed markedly. For example, compare regular patterns 2 and 3. As shown in Figure 7a, the flow is in the direction as shown over pattern 2. This represents a 3-by-3-foot section which was repeated eight times to form the entire roughness pattern for the 24 feet. The longitudinal and transverse spacings were 6 and 18 inches respectively, and the sum of these two was 24 inches. Roughness pattern 3 was formed by merely rotating pattern 2 counterclockwise 90°, as shown in Figure 7b. Roughness pattern 3 was formed by repeating this 3-foot section eight times over the 24 feet. The longitudinal and transverse spacings were 9 and 12 inches respectively, and the sum was 21 inches. In terms of rows and columns, pattern 2 can be considered a 2-by-6 (2 elements per row for 6 rows), and likewise pattern 3 can be considered as a 3-by-4. Even though both patterns have exactly the same roughness intensity, the flows will see markedly different spacings. Patterns 4 and 5, and patterns 6 and 7 were formed in a similar manner.

The derived constant resistance coefficients for each roughness pattern are plotted in Figure 8 against the associated roughness intensities. As clearly shown, significantly different resistance coefficients resulted for those patterns with the same roughness intensity. The resistance coefficients for the random patterns were the highest in all three cases. Roughness intensity did not adequately explain all of the variation in the resistance coefficient.

In an attempt to further explain the variation of resistance coefficient, a spacing parameter was formed:

$$\sigma = \frac{x + e}{h} \quad \ldots\ldots\ldots\ldots (23)$$

where x and e are the longitudinal and transverse spacing respectively, and h is the height of the hemispheres. This spacing parameter only has meaning for regularly spaced elements, since spacing for the random patterns is not regular. Resistance coefficients for the regular patterns were plotted against spacing parameter in Figure 9. Spacing parameter reduces much of the variation in resistance coefficient as related to roughness intensity. Also plotted on the curve formed by regular patterns are $\sqrt{f}$-values for random patterns. This was done to illustrate an "equivalent" spacing effect. For example, consider patterns 4, 7, and 8. All three had different roughness intensities (0.0966, 0.145 and 0.0645 respectively); however, essentially the same resistance coefficient resulted for all three patterns even though patterns 4 and 7 had the same spacing parameter. The particular random distribution of pattern 8 was hydraulically equivalent to the spacing of regular patterns 4 and 7.

The uniqueness of roughness intensity with element spacing in LBE streams, as shown by Judd and Peterson (7), suggests that the spacing arrangement could result in an optimal resistance. Nature develops some unique order of things in LBE streams. As shown in laboratory simulations here, when roughness intensity is held constant and spacing is varied, significantly different resistance coefficients resulted. Since the only variable is spacing, it follows that the term friction loss or friction coefficient is a serious misnomer, as Rouse (15) has suggested.

Let the total resistance coefficient be considered as the ratio of the head loss $H_1$ (in feet) divided by the velocity head $V^2/2g$ (in feet)

$$f/8 = \frac{H_2}{V^2/2g} \quad \ldots\ldots\ldots\ldots (24)$$

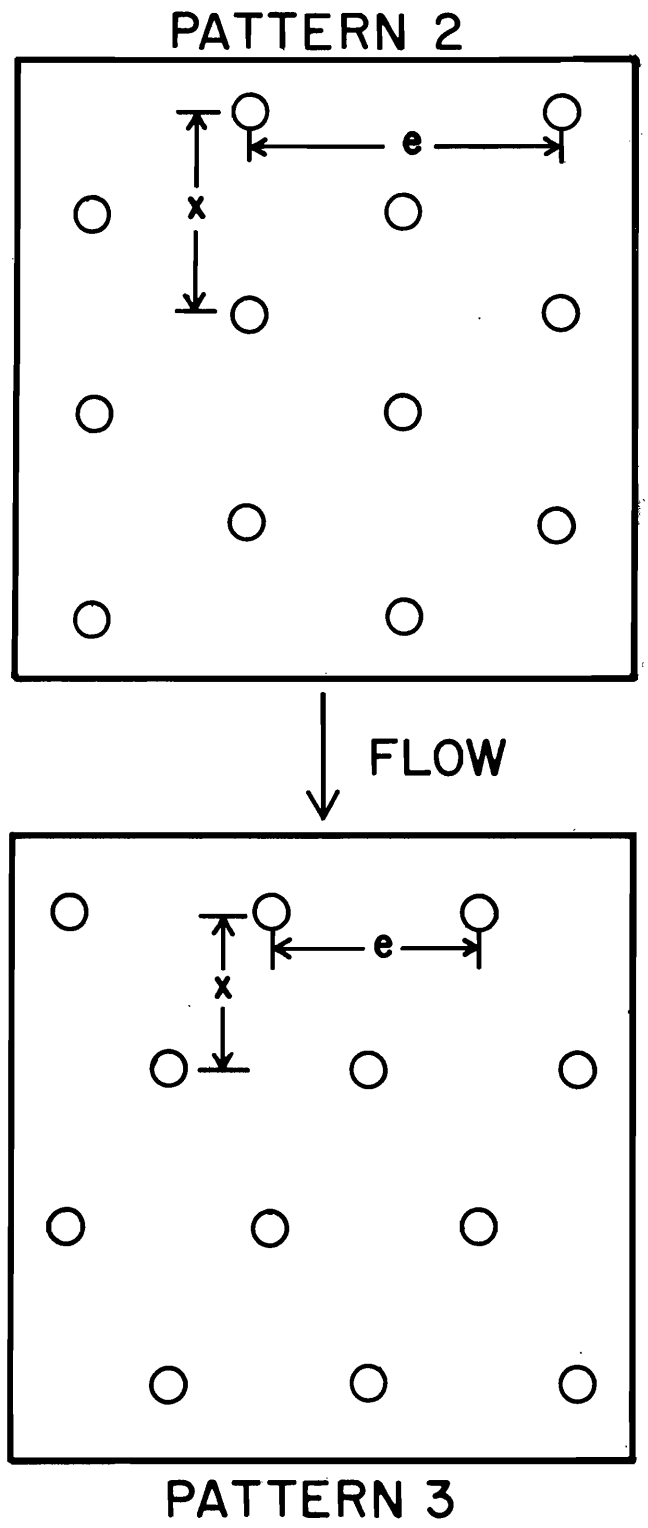


**Figure 7. Comparison between spacing of patterns 2 and 3.**

An increase in head loss going from a regular spacing to a random spacing can be computed as

$$H_l = \frac{f_{ran} - f_{reg}}{f_{reg}} \times 100\% \quad \ldots\ldots (25)$$

The increase in head loss due to randomness for each of these three groups of equal roughness intensities is,

| Patterns | Increase |
|---|---|
| 2,3,8 | 48% |
| 4,5,9 | 34% |
| 6,7,10 | 61% |

The spacing effect makes it difficult to correlate resistance coefficient with roughness intensity, and produces an added dimension of uncertainty in extrapolating laboratory relations to natural streams.

## Resistance Diagrams

The hydraulic data for the 14 LBE channels reported by Judd and Peterson (7) were analyzed by the numerical procedure reported by Overton and Hamon (11). A single resistance coefficient associated with a single plane of effective zero velocity was derived for each channel site. Pictures and associated site descriptions are reported in the paper by Judd and Peterson (7) and therefore will not be reproduced. All channels were considered to be essentially rectangular. For each of the channels, a plot of $Q/\sqrt{S}$ against $A\sqrt{8gR}$ has been made in Figures 10 through 23. The inverse of the slope of each regression line is the associated $\sqrt{f}$-value for each channel.

One other set of data has been analyzed in the present study, the data reported by the Corps of Engineers (5). These flows were measured in three rectangular flumes, 0.5 foot, 1 foot, and 2 feet wide. The flumes were roughened by concrete ridges 0.04 foot high placed perpendicular to the direction of flow and spaced at regular intervals. Resistance coefficients for these roughness patterns have been plotted against roughness intensities along with the previously analyzed data in Figure 24. The data points have been labeled with the ratio of the height of roughness elements, h, to the width of the flume, w. This parameter is referred to as the "wall effect ratio," h/w.

It appears that the resistance coefficient has a maximum value when roughness intensity is about 0.15. The results of the laboratory flume studies of Abdelsalam (1) and Kharrufa (8) with graded gravel elements have shown that resistance coefficient peaks out at a roughness intensity of about 0.10. Resistance coefficient then drops off rapidly and would theoretically approach a smooth

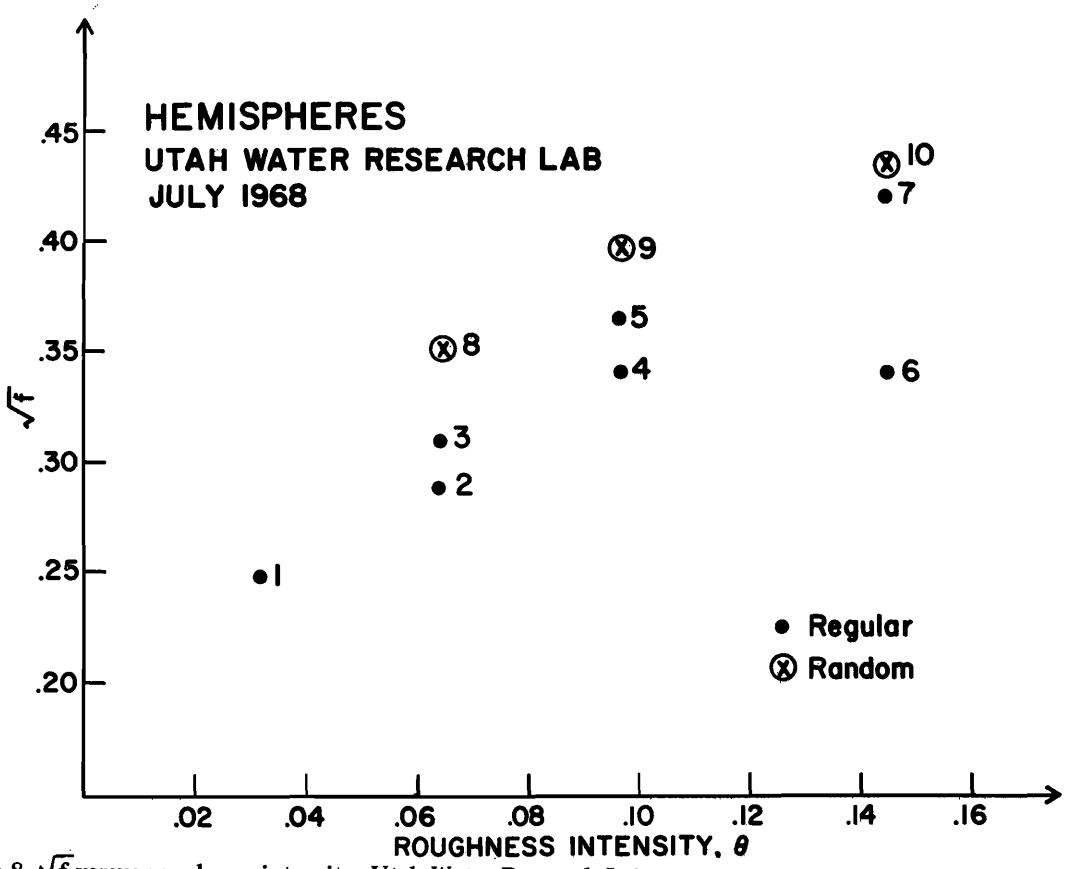


Figure 8. $\sqrt{f}$ versus roughness intensity, Utah Water Research Laboratory, July 1968.

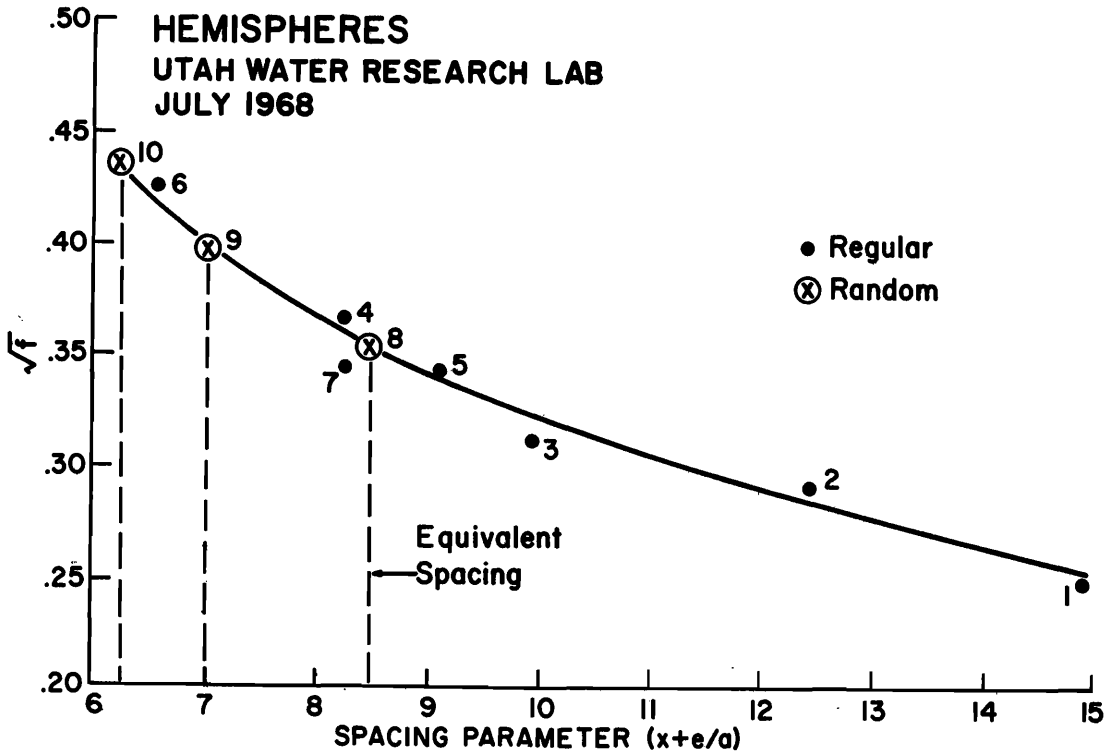


Figure 9. $\sqrt{f}$ versus spacing parameter, Utah Water Research Laboratory, July 1968.

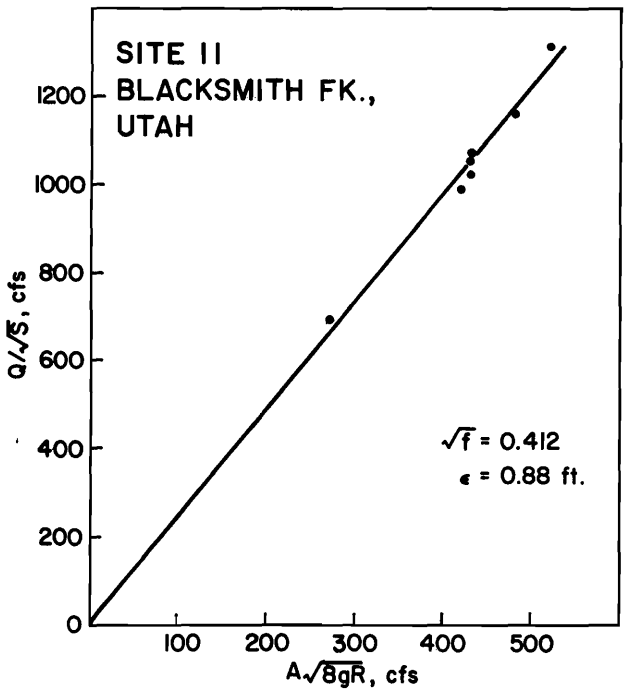


Figure 10. Derivation of constant resistance coefficient for LBE Site 11.

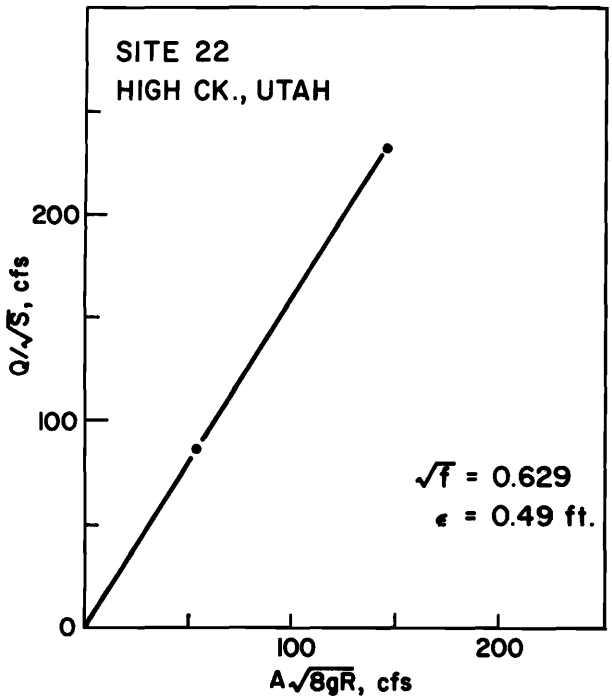


Figure 11. Derivation of constant resistance coefficient for LBE Site 22.

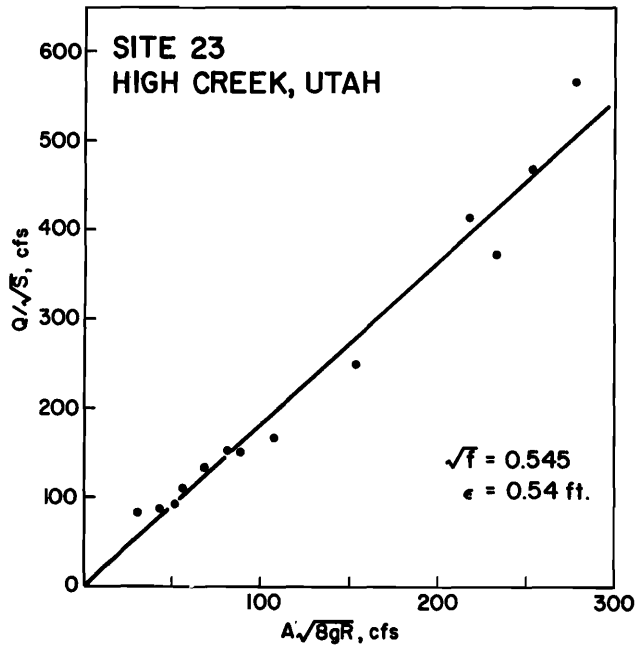


Figure 12. Derivation of constant resistance coefficient for LBE Site 23.

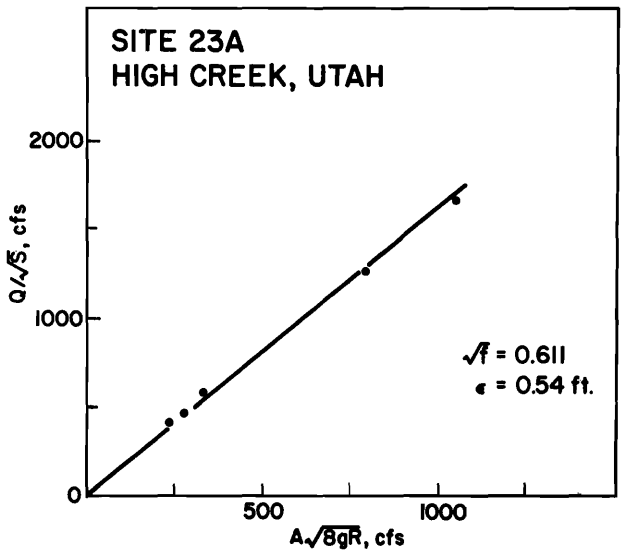


Figure 13. Derivation of constant resistance coefficient for LBE Site 23 A.

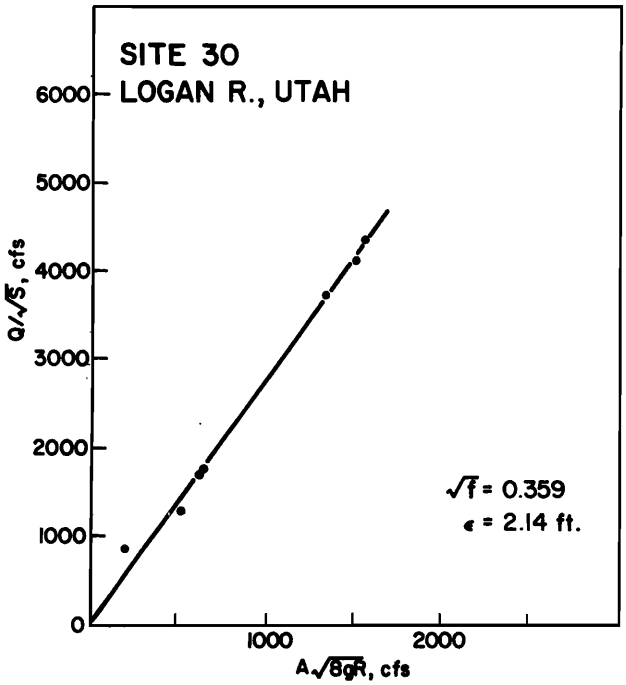


Figure 14. Derivation of constant resistance coefficient for LBE Site 30.

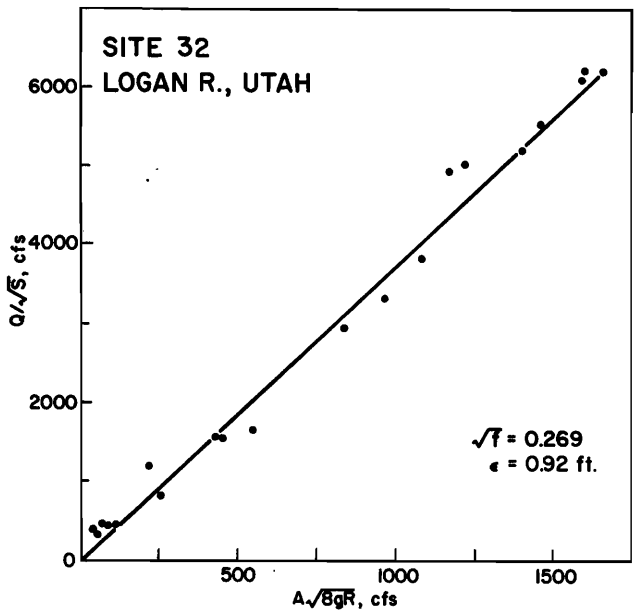


Figure 15. Derivation of constant resistance coefficient for LBE Site 32.

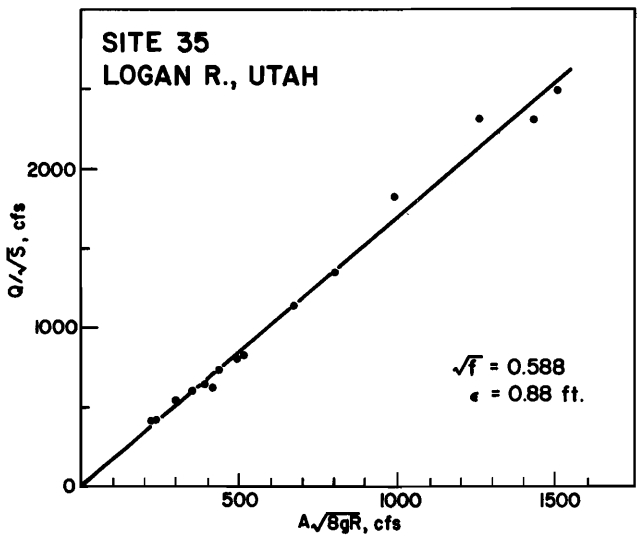


Figure 16. Derivation of constant resistance coefficient for LBE Site 35.

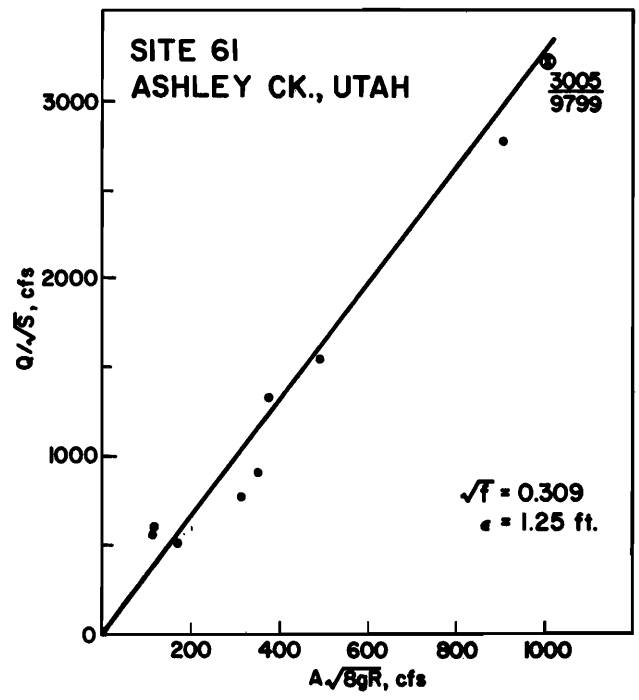


Figure 17. Derivation of constant resistance coefficient for LBE Site 61.

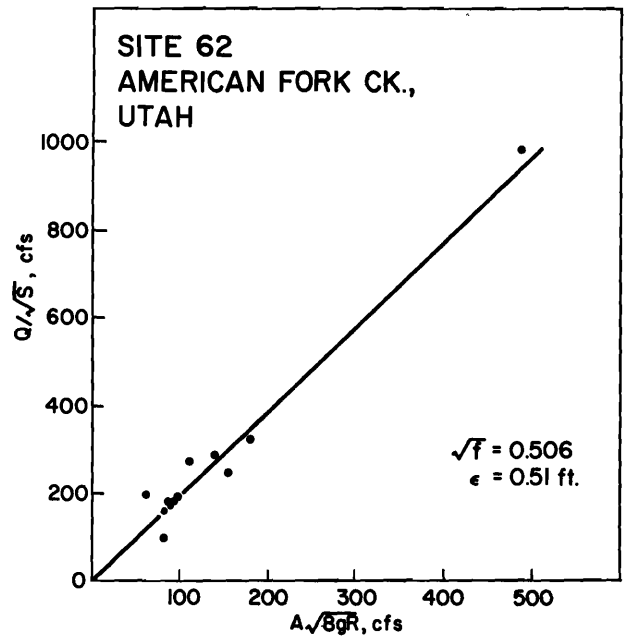


Figure 18. Derivation of constant resistance coefficient for LBE Site 62.

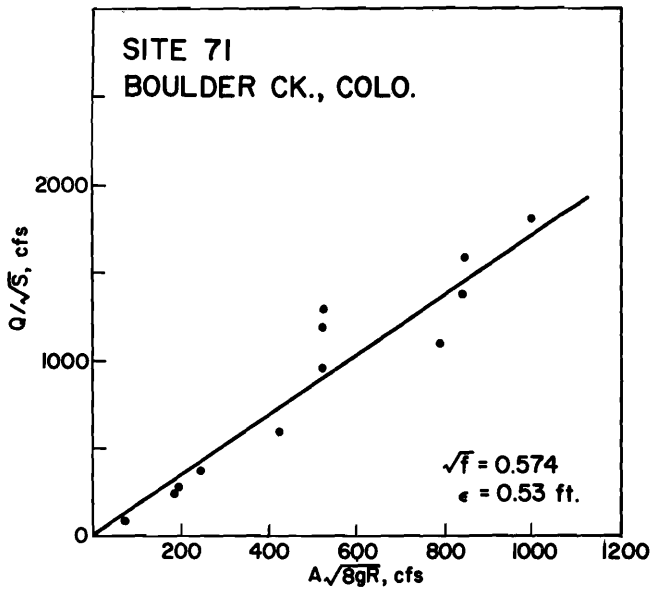


Figure 20. Derivation of constant resistance coefficient for LBE Site 71.

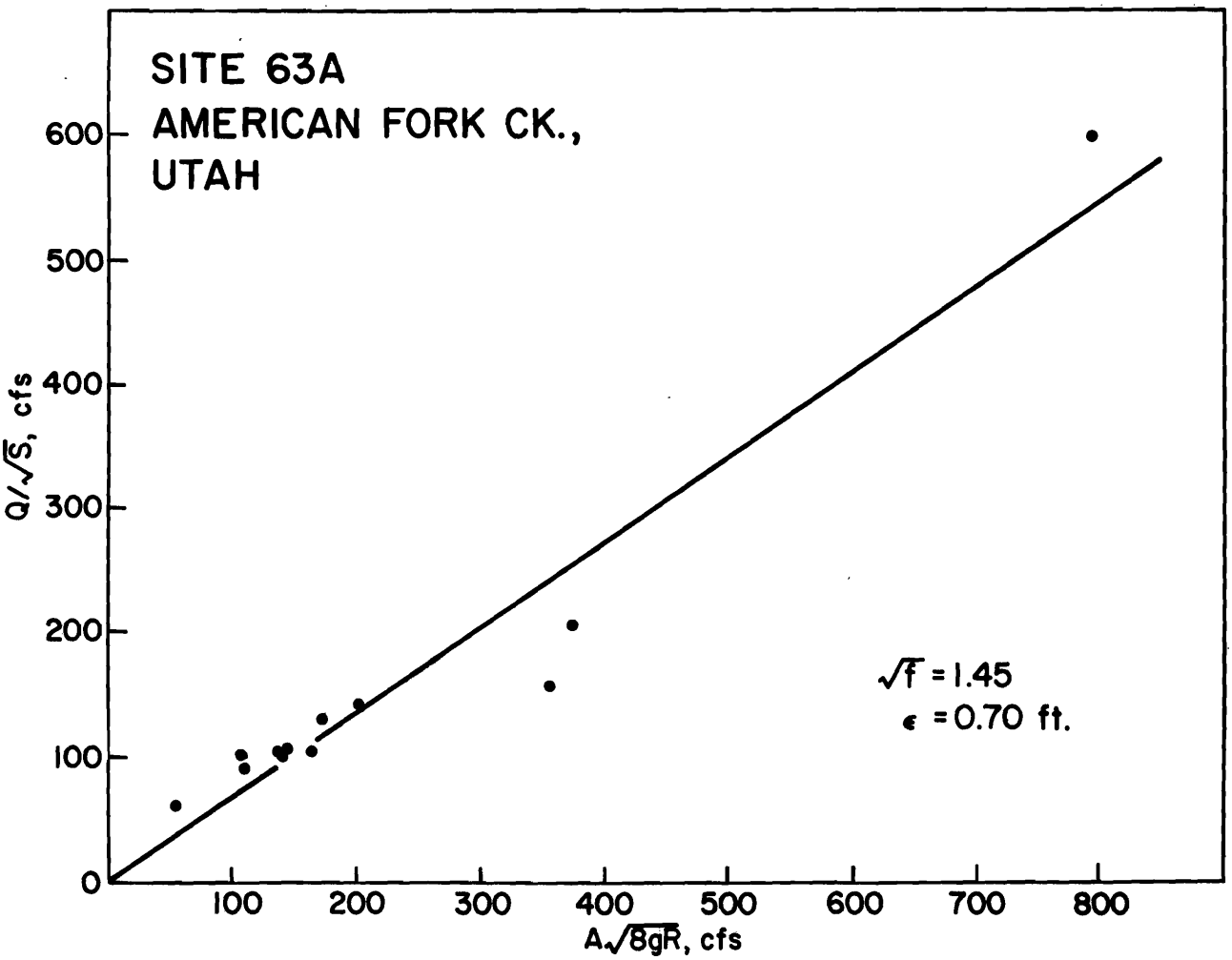


Figure 19. Derivation of constant resistance coefficient for LBE Site 63 A.

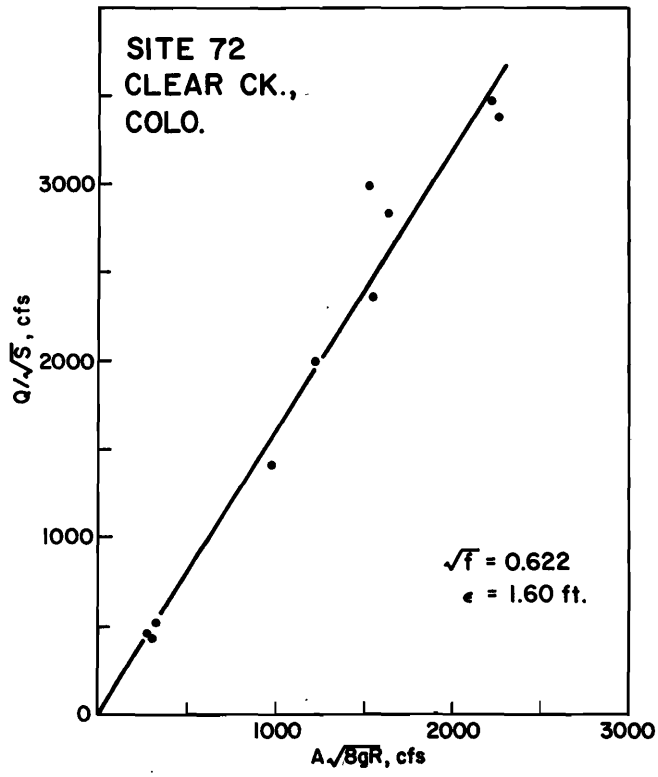


Figure 21. Derivation of constant resistance coefficient for LBE Site 72.

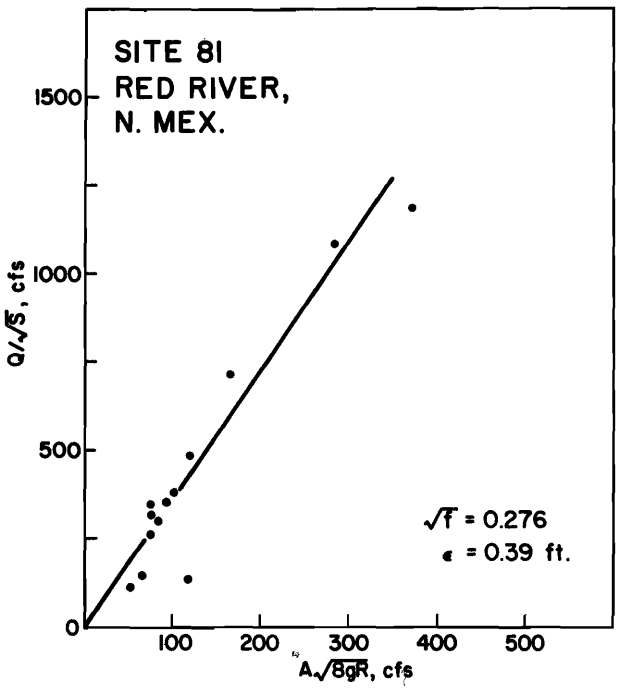


Figure 22. Derivation of constant resistance coefficient for LBE Site 81.

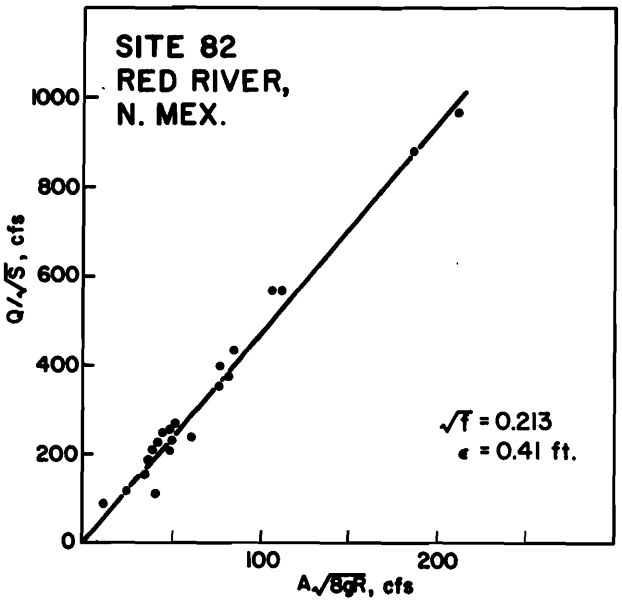


Figure 23. Derivation of constant resistance coefficient for LBE Site 82.

channel if the elements were placed closer together. In Figure 25, the solid lines are generalizations of the laboratory data shown in Figure 24. Resistance coefficients derived from the LBE streams have been plotted on this diagram also. There is little agreement between the LBE data and the laboratory data. Most of the LBE stream data occur between values of roughness intensity of 0.1 and 0.2. This may indicate that the resistance phenomenon illustrated by the solid lines does not occur in LBE streams. Roughness intensity is not the best geometric variable for explaining variation of the resistance coefficient in laboratory flumes. The spacing parameter developed in this report correlated with the resistance coefficient better than roughness intensity did.

An attempt was made to develop a diagram for the variation of the roughness parameter, i.e. height of plane of zero velocity above flume floor. This is shown in Figure 26. The ratio of the roughness parameter to the mean height of the LBEs has been plotted against roughness intensity and wall effect ratio is shown as a parameter. There was a stronger trend here than in the resistance coefficient diagram. Lines have been drawn in an attempt to generalize the results. As shown, the trend appears to be that the ratio of $\epsilon/k_{50}$ decreases as the wall effect ratio increases. A possible explanation for this occurrence will be offered.

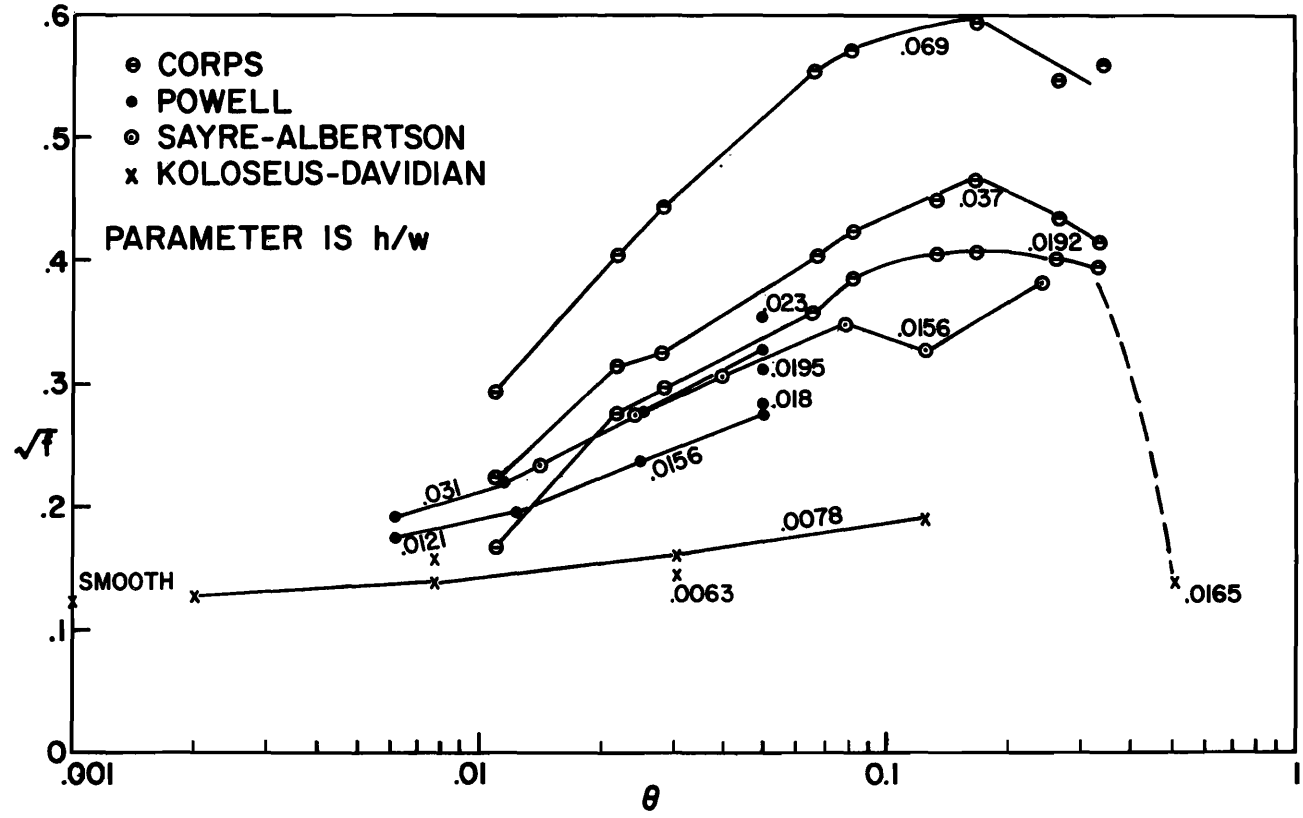


Figure 24. $\sqrt{f}$ versus roughness intensity for the previously published laboratory data.

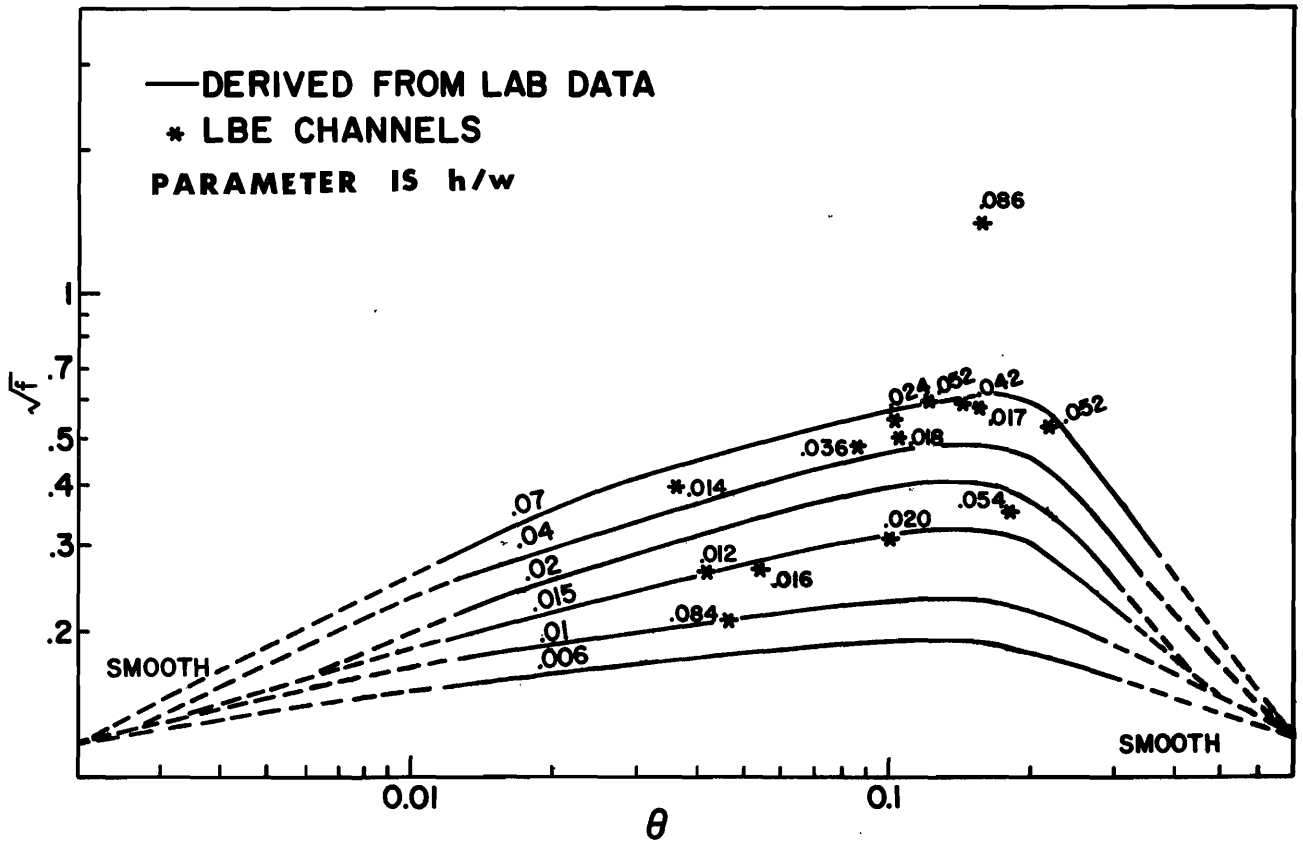


Figure 25. Resistance diagram developed from laboratory data applied to the LBE data.

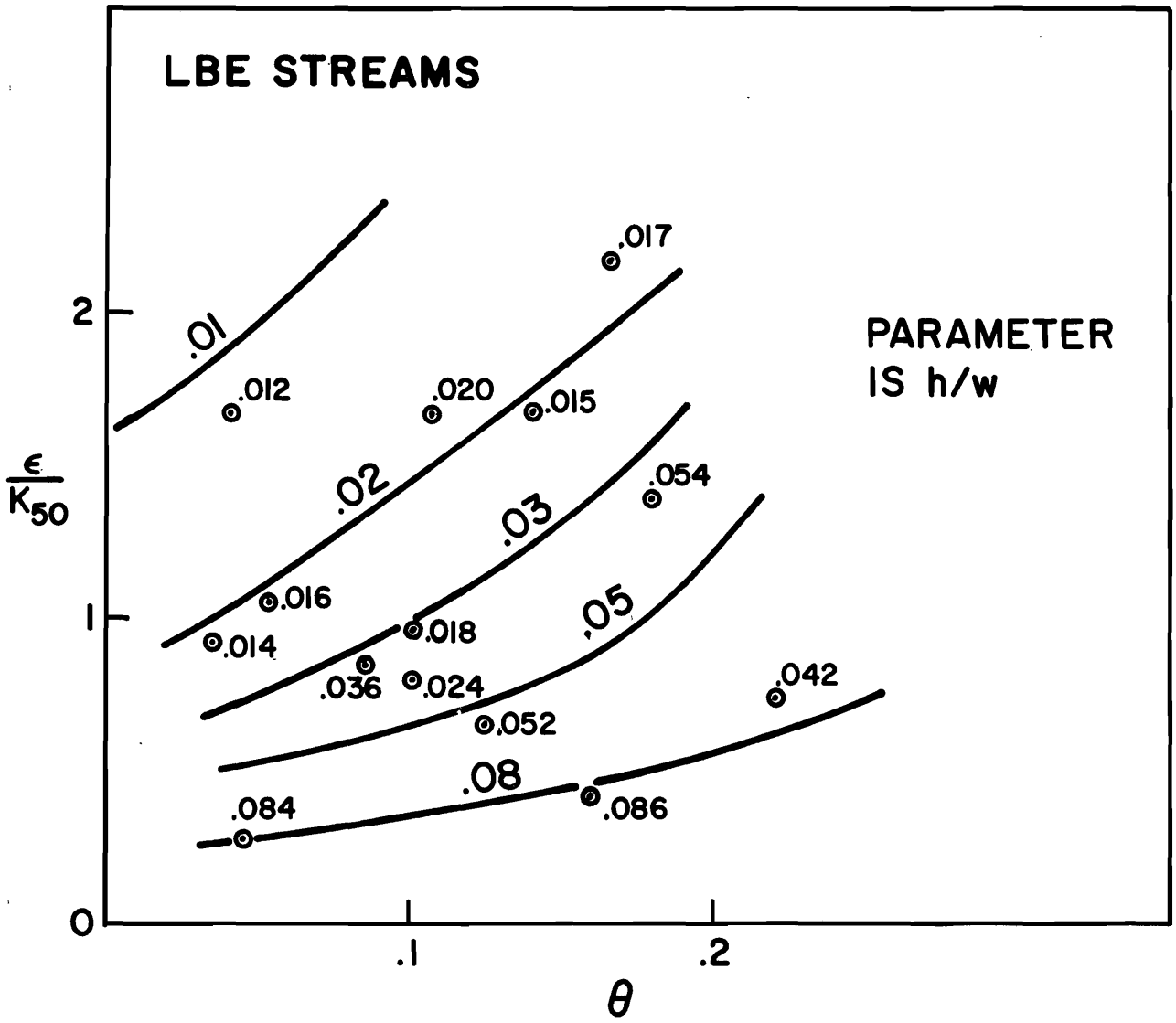


**Figure 26.** $\epsilon/K_{50}$ **for LBE streams.**

Consider two hypothetical streams with the same bed roughness intensity, the same average size material, but with different widths. The wall effect ratio of the narrower channel will be higher than the wall effect ratio of the wider channel. Figure 26 suggests that the $\epsilon/k_{50}$ ratio for the narrower channel will be less than the same ratio of the wider channel. With a greater wall effect relative to the resistance effect due to the size of the material there would be a greater degree of turbulence, thereby producing an increase in the movement of flows in the boundary layer. This could tend to place the plane of zero velocity to an elevation closer to the bottom of the channel.

## Summary and Conclusions

Two resistance diagrams have been developed from an analysis of previously reported laboratory data from rectangular flumes and from the analysis and data of LBE streams reported by Judd and Peterson (7). The Darcy–Weisbach resistance coefficient and the location of the plane of effective zero velocity have been related to the roughness intensity, the width of the channels, and the mean size of the material. Roughness intensity does not adequately explain the variation of the resistance coefficient in laboratory roughnesses, and spacing of the roughness elements is a more important factor. The streamflow regime appears to arrange the LBE in an optimal way. Roughness intensities of between 0.10 and 0.20 would appear to be realistic values for laboratory simulation of LBE streams. A clear cut similarity between laboratory and field data does not exist.

It is hoped that the results of this study can be of immediate use in design of stable channels, and that it may serve as a working similarity criterion for designing laboratory and field studies.

# REFERENCES


1. Abdelsalam, M. W. 1965. Flume study of the effect of concentration and size of roughness elements on flow in high gradient natural channels. Ph.D. dissertation, Utah State Univ., Logan, Utah.

2. Al-Khafaji, Abbas Nasser. 1961. The dynamics of two dimensional flow in steep, rough open channels. Ph.D. dissertation, Utah State Univ., Logan, Utah.

3. American Society of Civil Engineers. 1963. Friction factors in open channels: Progress report of the Task Force on Friction Factors in Open Channels of the Committee on Hydromechanics of the Hydraulics Division, Journal of the Hydraulics Division, ASCE 89(HY2):97-143.

4. Barnes, Harry K., Sr. 1967. Roughness characteristics of natural channels. U.S. Geological Survey, Water Supply Paper 1848, Washington, D.C.

5. Corps of Engineers. 1953. Roughness standards for hydraulic models. Report No. 1 Study of finite boundary roughness in rectangular flumes, Waterways Experiment Station, U.S. Army, Tech. Memo. No. 2-364, Vicksburg, Miss.

6. Hariri, Davoud. 1964. Relation between the pavement and the hydraulic characteristics of non-cohesive high-gradient channels. Ph.D. dissertation, Utah State Univ., Logan, Utah.

7. Judd, Harl E. and Dean F. Peterson. 1969. Hydraulics of large bed element channels. PRWG 17-6, Utah Water Research Laboratory, College of Engineering, Utah State Univ., Logan, Utah.

8. Kharrufa, Najib S. 1962. Flume studies of flow in steep, open channels with large, graded, natural roughness elements. Ph.D. dissertation, Utah State Univ., Logan, Utah.

9. Koloseus, H. J. and Jacob Davidian. 1966. Free surface instability correlations. Laboratory Studies of Open Channel Flow, U.S. Geological Survey Water Supply Paper 1592C, Washington, D.C.

10. Mohanty, P. K. 1959. The dynamics of turbulent flow in steep, rough, open channels. Ph.D. dissertation, Utah State Univ., Logan, Utah.

11. Overton, D. E. and W. Russell Hamon. 1970. Optimizing resistance coefficients in open channels. Unpublished report. Agricultural Research Service, Boise, Idaho.

12. Peterson, Dean F. and P. K. Mohanty. 1960. Flume studies in steep, rough channels. Proceedings, Journal of Hydraulics Division, ASCE 86(HY9):55-76.

13. Powell, Ralph W. 1946. Flow in a channel of definite roughness. ASCE Transactions, 111:531-566.

14. Ragan, R. M. 1965. Synthesis of hydrographs and water surface profiles for unsteady open channel flow with lateral inflows. Ph.D. dissertation, Cornell Univ., Ithaca, N.Y.

15. Rouse, Hunter. 1965. Critical analysis of open channel resistance. Journal of Hydraulics Division, ASCE 91(HY4):1-25.

16. Sayre, William W. and Maurice L. Albertson. 1961. Roughness spacing in rigid open channels. Journal of Hydraulics Division, ASCE 87(HY3):121-150.

17. Tracy, H. J. and C. M. Lester. 1961. Resistance coefficients and velocity distribution in a smooth rectangular channel, laboratory studies of open channel flow. U.S. Geological Survey Water Supply Paper 1592-A, Washington, D.C.